

FILE COPY
NO. 3

★
**CASE FILE
COPY**

TECHNICAL MEMORANDUMS

NATIONAL ADVISORY COMMITTEE FOR AERONAUTICS

No. 738

INVESTIGATION OF A RATEAU SUPERCHARGER FOR
A 700-HORSEPOWER AIRPLANE ENGINE

By Hermann Oestrich

Automobiltechnische Zeitschrift
August 25, 1933

THIS DOCUMENT ON LOAN FROM THE FILES OF
NATIONAL ADVISORY COMMITTEE FOR AERONAUTICS
LANGLEY AERONAUTICAL LABORATORY
LANGLEY FIELD, HAMILTON, VIRGINIA

RETURN TO THE ABOVE ADDRESS.
REQUESTS FOR PUBLICATIONS SHOULD BE ADDRESSED
AS FOLLOWS:
NATIONAL ADVISORY COMMITTEE FOR AERONAUTICS
1724 F STREET, N.W.
WASHINGTON 25, D.C.

Washington
March 1934

NATIONAL ADVISORY COMMITTEE FOR AERONAUTICS

TECHNICAL MEMORANDUM NO. 738

INVESTIGATION OF A RATEAU SUPERCHARGER FOR

A 700-HORSEPOWER AIRPLANE ENGINE*

By Hermann Oestrich

I. DESCRIPTION

This supercharger is designed for supercharging a 12-cylinder water-cooled engine of 720 hp. at 1,700 r.p.m. It is a two-stage centrifugal compressor driven by the engine through a Farman clutch. Its chief characteristics are:

Delivery,	0.67 kg/s	1.48 lb./sec.
Pressure,	1,033 abs. atm.	15.185 lb./sq.in.
Speed,	1,700 r.p.m.	
Compression ratio,	2	
Type of supercharger,	centrifugal compressor	
Gear ratio,	12.3	
Type of rotor,	open on both sides	
Number of stages,	2	
	<u>Stage 1</u>	<u>Stage 2</u>
Number of rotor vanes,	9	9
Number of guide vanes,	none	none
Outlet diameter of rotor,	260 mm (10.24 in.)	260 mm (10.24 in.)
Inlet diameter of rotor,	164 mm (6.46 in.)	152 mm (5.98 in.)

*"Untersuchung eines Aufladers für einen 700-PS-Flugmotor." Automobiltechnische Zeitschrift, August 25, 1933, pp. 405-411.

	Stage 1	Stage 2
Inlet angle β_1 at rotor	90°	90°
Outlet angle β_2 at rotor	90°	90°
Width of vane passage at outlet	18.0 mm (0.71 in.)	16.0 mm (0.63 in.)
Width of vane passage at inlet with $d=180$ mm (7.1 in.) (stage 1) and $d=170$ mm (6.7 in.) (stage 2)	32.5 mm (1.28 in.)	31.0 mm (1.22 in.)
Outlet angle of inlet guiding apparatus at maximum inlet diameter of rotor	38°	46°

Further details are shown in figures 1 to 7. See figure 3 for table of dimensions.

II. TESTING

For more thorough investigation, the supercharger was mounted on the test stand of the DVL (Deutsche Versuchsanstalt für Luftfahrt). In order to produce the condition of operation at high altitudes, the air inlet was throttled. On the outlet side, the air was conducted through a short wide stack into the open. The tests were made with the following instruments and methods:

Air measurement: 1912 standard nozzle, diameter 120 mm (4.72 in.).

Torque: cradle-type dynamometer.

Revolution speed: DVL tachometer.

Inlet pressure: U-tube with mercury.

Outlet pressure: U-tube with water.

Inlet temperature: alcohol thermometer.

Outlet temperature: thermocouple.

Several series of tests were made, in which the r.p.m. was gradually increased. Each reading was taken after the

torque had become constant. A constant inlet temperature was not awaited, so that the outlet temperatures had to be correspondingly corrected.

The measured values are given in table I. With their help the work diagram of the supercharger (fig. 8) was plotted in the usual manner. It is valid for an intake temperature of 20°C . (68°F .) and a final pressure of 1,033 abs. atm. (15.185 lb./sq.in.), and shows the relation between quantity delivered, compression ratio, r.p.m., power required, and efficiency. If the intake temperature of the supercharger is altered, the compression ratio at a given r.p.m. is also altered. The compression ratio at another intake temperature is determined on the basis of the fact that the adiabatic delivery head for the volume delivered is nearly constant.* A work diagram of general application is therefore obtained if, instead of the coordinates of figure 8, the volume delivered, based on the intake condition, is chosen as the abscissa and the effective adiabatic delivery head as the ordinate, as was done in figure 9. In the latter figure the lines of constant revolution speed and constant efficiency are, within broad limits, independent of the intake pressure and temperature. The other lines are valid for a final pressure of 760 mm (29.9 in.) Hg and a relation between the intake pressure and temperature corresponding to that in the CINA (Committee Internationale de Navigation Aerienne) standard atmosphere.

By the adiabatic delivery head is meant the amount of energy required for the adiabatic compression of one kilogram of the air to the desired final pressure. For the adiabatic delivery head H_{ad} in the compression from the pressure p_1 to the pressure p_2 , with the customary notation in thermodynamics, we have

*This restriction must be made because the volume delivered varies during the compression and the proportional variation is also affected by the compression ratio. Hence the air velocities at the rotor inlet and outlet, which decide the delivery head, cannot be fully and definitely determined from the rotor r.p.m. and intake volume.

$$H_{ad} = R T_1 \frac{x}{x-1} \left[\left(\frac{p_2}{p_1} \right)^{\frac{x-1}{x}} - 1 \right] \text{ m } \frac{\text{kg}}{\text{kg}}$$

With this equation the compression ratio p_2/p_1 at a given intake temperature can therefore be calculated from the adiabatic delivery head H_{ad} and the intake temperature T_1 . In order to simplify the determination of the compression ratio, the function

$$\frac{H_{ad}}{T_1} = R \frac{x}{x-1} \left[\left(\frac{p_2}{p_1} \right)^{\frac{x-1}{x}} - 1 \right] \frac{\text{m}}{^\circ\text{C}}$$

was plotted in figure 10. After the delivery head has been determined from figure 9 for a certain operating condition, the corresponding compression ratio is then obtained by dividing the delivery head by the absolute intake temperature and introducing the quotient into figure 10.

In superchargers the constant-pressure altitude is just as important as the compression ratio. By this is meant the altitude up to which the supercharger is able to compress the air to the pressure at sea level.

The difference between the adiabatic delivery head and the constant-pressure altitude is small. The explanation of this is simple. The existence of equilibrium in the atmosphere is based on the assumption that the compression energy absorbed by one kilogram of air in passing from the altitude H_1 to the altitude H_2 , under constant heat exchange with the environment, must equal the energy given off by it due to the change in altitude.

If $H_2 = 0$, then

$$H_1 = \int_1^0 v \, dp = \int_1^0 \frac{dp}{\gamma}$$

where the relation prevailing in the atmosphere at the time must be inserted between p and v . If the relation is inserted which was established by the CINA for the stand-

ard atmosphere on the basis of numerous experiments, H_1 represents the CINA altitude corresponding to air condition 1.

Since, in the compression on the basis of the relation between p and v in the CINA atmosphere, the temperature of the air increases, although not so much as in the adiabatic compression, the geometric altitude H_1 , at which the air is in the condition 1, must be lower than the adiabatic but higher than the isothermal delivery head requisite for its compression to the atmospheric pressure at sea level.

Figure 11 represents the relation between the CINA constant-pressure altitude and the requisite delivery head for attaining this altitude. In order to enable an accurate reading in a small space, the difference between the adiabatic delivery head and the corresponding CINA constant-pressure altitude was plotted against the CINA altitude and the adiabatic delivery head. It is seen that the difference is very slight, especially for altitudes below 6,000 m (19,685 ft.). Figure 11 also contains the decrease in the absolute temperature T and the relative decrease in the air pressure p and the air density γ plotted against the CINA altitude.

With the aid of these relations, the CINA constant-pressure altitude and the corresponding CINA compression ratio, for a given revolution speed and quantity delivered, can be immediately determined from figure 9. In order to enable a quick approximation of these values from figure 9, the CINA constant-pressure altitudes corresponding to the adiabatic delivery head and the corresponding CINA compression ratio were plotted on a special scale of ordinates. Figure 9 also contains the lines of constant power and delivery weight resulting from normal atmospheric conditions and a final pressure of 760 mm Hg. These lines, as likewise the special ordinate scales, are therefore valid only for the case where the same relation exists between temperature and pressure in the CINA atmosphere and where the final pressure is equivalent to 760 mm Hg in contrast with the lines of constant revolution speed and efficiency, which are independent of the initial temperature and pressure and always remain practically constant.*

*Slight variations in the adiabatic efficiency are due to the fact that the mechanical-friction losses do not vary according to the power required for the compression. See footnote, page 3, regarding slight variations in adiabatic delivery head.

The delivery weight G and the required power N can generally be calculated from

$$G = V_1 \gamma_1 = V_1 0.464 \frac{b_1}{T_1} \text{ kg/s}$$

and

$$N = G \frac{H_{\text{eff}}}{75 \eta_{\text{ad}}} \text{ hp.}$$

where b denotes the aerodynamic pressure in millimeters of mercury and the subscript 1 refers to the intake condition.

The power curves in figures 8 and 9 show that the best adiabatic efficiency is somewhat above 54 percent and is attained at 1,400 r.p.m. and for a delivery of $0.775 \text{ m}^3/\text{s}$ (27.37 cu.ft.) (based on the intake condition), the adiabatic delivery head being 4,900 m ($16,076 \text{ ft.}$) and the corresponding CINA compression ratio 1.81. For normal operation ($n = 1700 \text{ r.p.m.}$ and $G = 0.67 \text{ kg/s}$ (1.48 lb./sec.)), the adiabatic efficiency $\eta_{\text{ad}} = 52$ percent, the adiabatic delivery head $H_{\text{ad}} = 6,500 \text{ m}$ ($21,325 \text{ ft.}$), the CINA constant-pressure altitude $H_{\text{CINA}} = 6,240 \text{ m}$ ($20,472 \text{ ft.}$) and the CINA compression ratio $(p_o/p)_{\text{CINA}} = 2.22$.

In order to understand the flow conditions in the supercharger, the air velocities at various points, the theoretical delivery heads and several characteristics are given in table II. Of the theoretical delivery heads, only those obtained without guide vanes can be accurately determined. It appears hopeless to try to calculate the influence of the guide vanes on the delivery head for any given delivery quantity, because the flow conditions in the guiding apparatus are so unsettled. This also accounts for the inability to calculate the delivery quantity for undisturbed inflow. Judging from the angles of the inflow guide vanes, the delivery quantity under normal operating conditions seems to be less than for undisturbed inflow and the same revolution speed.

For the delivery quantity with undisturbed inflow into the rotor, the theoretical delivery head could be calculated on the basis of an assumption more clearly designated in table III

III. SUMMARY

The Rateau supercharger investigated had, under normal operating conditions ($n = 1,700$ r.p.m. and $G = 0.67$ kg/s), an adiabatic efficiency of 52 percent, the CINA constant-pressure altitude being 6,240 m (20,472 ft.) and the corresponding CINA compression ratio being 2.22. Its best adiabatic efficiency was 54 percent at 1,400 r.p.m. and with a delivery quantity of 0.77 m³/s. The power required under normal running conditions was 110 hp. In order to understand the flow conditions in the supercharger, the air velocities at various points, the theoretical delivery heads and a few characteristics were calculated.

IV. APPENDIX

Calculation of the Mean Inlet Diameter

The mean inlet diameter is necessary to determine the theoretical delivery head with undisturbed inflow. In this case the generally valid formula, for a blower with radial vanes at inlet and outlet, is

$$H_{\text{theor. } \infty} = \frac{1}{g} (u_2^2 - u_1^2) \quad (1)$$

In the blower investigated, the inflow into the rotor does not occur at a certain definite diameter D_1 , but, as shown in figure 12, at diameters between D_3 and D_4 , i.e., on an annular opening. The peripheral velocities therefore lie between u_3 and u_4 .

Table I. Experimental values

Date: Aug. 12, 1931.

Oil temperature: 50 to 60°C

Barometer: 758.2 mm Hg

Oil pressure: 2 to 3 atm.

No.	Time	Throttle position	Revolution speed	Corrected torque	Pressure before supercharger	Pressure behind nozzle	Pressure difference in nozzle	Temperature air inflow *	Temp. increase of air in superch'gr.	
									Begin'g.	End of experiment
	h:min.		r.p.m.	\times .537 mkg	mm Hg neg. pres.	mm H ₂ O neg. pres.	mm H ₂ O	Degrees centigrade		
1		50	1000	49.0	151	185	155	20	31.7	
2		50	1163	60.5	189	228	194		43.2	
3		35	1008	49.0	154	182	154		32.8	
4		10	1170	50.1	240	116	96		49.5	
5		10	1340	61.3	296	130	110			
6		10	1520	70.2	340	142	120			
7		10	1595	74.9	363	149	124			
8		10	698	22.1	102	50	43	20	19.0	
9		10	902	33.8	160	78	67	20	29.3	30.5
10		10	1112	47.5	221	104	88	20	43.8	45.2
11		10	1320	58.7	288	122	104	20	62.5	66.0
12		10	1450	66.5	325	135	116	20	77.2	79.5
13		10	1705	80.6	384	150	126	20	103.0	107.0
14	2 46	15	702	23.2	92	75	63	21	23.3	21.2
15		15	925	38.0	149	121	102	21.5	29.3	30.5
16		15	1093	50.3	195	169	135	21.5	41.4	41.4
17		15	1247	61.5	232	189	158	21.5	54.2	55.3
18		15	1395	72.8	272	218	185	21.5	66.0	67.7
19	2 57	20	710	24.2	93	85	74	21.5	15.5	15.5
20	3 02	20	917	38.7	142	136	115	21.3	25.8	25.8
21	3 03	20	1092	52.1	187	180	154	21.0	37.4	38.7
22		20	1318	69.9	241	230	197	21.0	55.3	57.6
23	3 06	20	1310	70.1	242	232	198	21.0	58.7	58.7
24	3 14	35	665	22.8	84	83	70	20.5	16.3	16.3
25	3 16	35	905	39.5	135	144	121	20.3	23.3	23.3
26	3 17	35	1080	52.8	178	191	163	20.2	36.2	37.4
27	3 20	35	1328	71.6	232	247	212	20.2	54.2	55.2
28	3 22	70	713	25.2	91	91	79	20.4	21.1	
29	3 24	70	912	39.5	137	146	123	20.3	25.8	25.8
30	3 26	70	1090	53.0	180	196	167	20.2	35.2	37.0
31	3 28	70	1208	62.6	206	222	190	20.0	45.0	46.2
32	3 32	8	688	17.8	107	26	24	20.0	28.1	24.7
33	3 34	8	947	30.1	186	41	34	20.0	35.2	37.4
34	3 36	8	1115	37.3	236	48	42	20.0	48.3	50.7
35	3 37	8	1332	46.9	310	51	44	20.0	70.5	75.0
36	3 39	8	1540	54.7	366	54	46	20.0	95.5	101.0
37		8	1760	63.2	430	54	47	20.0	125.0	136.0
38	3 44	9	698	19.6	106	39	32	20.3	28.1	24.7
39	3 47	9	937	31.7	174	60	53	20.3	34.0	35.2
40	3 48	9	1090	40.7	225	73	64	20.0	44.9	46.2
41	3 51	9	1340	54.1	300	90	76	20.2	66.0	68.5
42		9	1505	63.3	353	100	85	20.2	86.3	89.7
43	3 55	9	1765	74.7	415	107	90	20.5	113.0	118.5
44		10	1735	82.6	402	148	125	20.3	106.0	113.0

* Simultaneous temperature of air in nozzle

$$\text{mkg} \times 7.23298 = \text{ft.-lb.}$$

TABLE II. Investigation of Flow Conditions

	Symbols	Operating conditions		
		Normal	Best efficiency	
a) <u>Air velocity</u>				
<u>1. Supercharger inflow and outflow</u>				
Intake air volume	V_e	1.05	0.775	kg/s
Revolution speed	n_a	1700	1400	r.p.m.
CINA constant-pressure altitude	H_{CINA}	6240	4750	m
CINA compression ratio	$\left(\frac{P_o}{P}\right)_{CINA}$	2.22	1.81	-
Adiabatic efficiency	η_{ad}	0.52	0.54	-
Mechanical efficiency of supercharger including drive, assumed	η_m	0.90	0.90	-
Hydraulic efficiency, based on adiabatic performance	$\eta_{hyd.ad.}$	0.577	0.60	-
Relative temperature increase, adiabatic	$\left(\frac{T}{T}\right)_{ad}$	1.258	1.1865	-
Relative temperature increase, effective (with $\eta_{hyd.ad.}$ calculated)	$\left(\frac{T}{T}\right)_{eff}$	1.447	1.311	-
Resulting compression exponent	n	1.86	1.84	-
Intake temperature (corresponding to CINA constant-pressure altitude)	T_e	247.5	257	°K
Outflow temperature (calculated)	T_a	358	337	°K

TABLE II (continued)

	Symbols	Operating conditions		
		Normal	Best efficiency	
Air density ratio $\frac{\gamma}{\gamma} = \left(\frac{p}{p}\right) \frac{1}{n}$	$\left(\frac{\gamma}{\gamma}\right)_{\text{eff}}$	1.535	1.381	-
Outflowing air volume	V_a	0.683	0.562	m ³ /s
Inflow section of supercharger	F_e	123	123	cm ²
Outflow " " "	F_a	95	95	cm ²
Inflow velocity of air	c_e	85.3	63	m/s
Outflow " " "	c_a	72	59.1	m/s
<u>2. Stage 1</u>				
Axial flow section before entrance to first rotor	F'_{ax}	179	179	cm ²
Mean axial-flow velocity	c'_{axm}	58.7	43.3	m/s
Flow section in rotor at r = 90 mm (3.54 in.)	F'_{90}	174	174	cm ²
Flow volume at rotor inlet (r = 90 mm)	V'_{90}	1.05	0.775	m ³ /s*
Relative velocity in rotor (r = 90 mm)	w'_{90}	60.3	44.5	m/s
Flow section at rotor outlet	F'_2	146	146	cm ²
Flow volume " " "	V'_2	0.928	0.709	m ³ /s*
Relative velocity at rotor outlet	w'_2	63.5	48.6	m/s

*See table III.

TABLE II (continued)

	Symbols	Operating conditions		
		Normal	Best efficiency	
<u>3. Stage 2</u>				
Axial flow section before inlet to second rotor	F''_{ax}	141	141	cm ²
Volume of flowing air	V''_{ax}	0.830	0.652	m ³ /s*
Mean axial velocity	c''_{axm}	58.8	46.2	m/s
Flow section in rotor (r = 85 mm) (3.35 in.)	F''_{85}	158	158	cm ²
Flow volume in rotor (r = 85 mm)	V''_{85}	0.830	0.652	m ³ /s*
Relative velocity in rotor (r = 85 mm)	w''_{85}	52.5	41.2	m/s
Flow section at rotor outlet	F''_2	130	130	cm ²
Flow volume " " "	V''_2	0.750	0.603	m ³ /s*
Relative velocity at rotor outlet	w''_2	57.7	46.3	m/s
<u>b) Delivery heads</u>				
Effective delivery head (adiabatically calculated)	H_{eff}	6500	4900	m
Peripheral velocity at outlet of stages 1 and 2	u_2	284.5	234.5	m/s
Theoretical delivery heads without guide vanes, with infinite number of rotor vanes	$H_{theor.∞}$	16450	11150	m

*See table III.

TABLE II (continued)

	Symbols	Operating conditions			
		Normal	Best efficiency		
b) Delivery heads (cont.)					
Minimum power factor for finite number of vanes according to Pfleiderer	$\frac{1}{\epsilon}$	1.467	1.467	-	
		to 1.583	to 1.583	-	
Theoretical delivery head without guide vanes, with 9 rotor vanes	$H_{theor.}$	11220	7620	m	
		to 10380	to 7030		
Mean peripheral velocity at rotor inlet, stage 1	$u' l_m$	142.5	117.7	m/s*	
Mean peripheral velocity at rotor inlet, stage 2	$u'' l_m$	134.2	110.7	m/s*	
Theoretical delivery head with undisturbed inflow, rotor vanes ∞	$H_{theor. \infty}$	12560	8530	m	
Theoretical delivery head with undisturbed inflow, rotor vanes 9	$H_{theor.}$	8560	5820	m	
		to 7930	to 5390	m	
c) Coefficients					
Load characteristics					
$\delta = \frac{V_2}{u_2 R_2^2}$	δ				
		Stage 1:	0.193	0.179	-
		Stage 2:	0.156	0.154	-
Pressure-head characteristics					
$\mu = \frac{H_{off}}{\frac{1}{g} \sum u_2^2}$	μ	0.395	0.440	-	

*See Appendix.

TABLE III. Calculation of Flowing-Air Volumes
at Various Points in the Supercharger

The calculation of these volumes is necessary, in order to determine the air velocities at the different points. It started with the assumption that the temperature increase of the air is the same in each stage and that the temperature increase in the rotor is half that in the whole stage.

$$1) n_a = 1,700 \text{ r.p.m.}; \quad V_e = 1.05 \text{ m}^3/\text{s}; \quad G = 0.67 \text{ kg/s};$$

$$T_e = 247.5 \text{ }^\circ\text{K}; \quad p_a/p_e = 2.22; \quad n = 1.86$$

	T/T_e	γ/γ_e	V
Supercharger inlet	1	1	1.05
Rotor 1, inlet	1	1	1.05
" 1, outlet	1.112	1.131	0.928
" 2, inlet	1.224	1.265	0.830
" 2, outlet	1.336	1.400	0.750
Supercharger outlet	1.447	1.535	0.683

$$2) n_a = 1,400 \text{ r.p.m.}; \quad V_e = 0.775 \text{ m}^3/\text{s}; \quad G = 0.587 \text{ kg/s};$$

$$T_e = 257 \text{ }^\circ\text{K}; \quad p_a/p_e = 1.81; \quad n = 1.84$$

	T/T_e	γ/γ_e	V
Supercharger inlet	1	1	0.775
Rotor 1, inlet	1	1	0.775
" 1, outlet	1.078	1.0935	0.709
" 2, inlet	1.156	1.1885	0.652
" 2, outlet	1.234	1.284	0.603
Supercharger outlet	1.311	1.381	0.562

The theoretical delivery head for the rotor of the blower investigated is therefore

$$H_{\text{theor. } \infty} = \frac{1}{g} \left(u_2^2 - \frac{\int^4 u^2 dG}{G} \right) \quad (2)$$

If $\frac{\int^4 u^2 dG}{3G} = u_{1m}^2$, then $u = r\omega$, the square of the mean inlet radius

$$r_{1m}^2 = \frac{\int^4 r^2 dG}{3G} \quad (3)$$

Over the inlet cross section $\gamma = \text{constant}$ (approximately). Then equation (3) becomes

$$r_{1m}^2 = \frac{\int^4 r^2 dV}{3V} \quad (4)$$

where $V = \frac{G}{\gamma}$ denotes the flowing volume.

Now $dV = c_{ax} dF = d\pi r^2 = 2\pi r dr$. Hence

$$r_{1m}^2 = \frac{2\pi \int^4 c_{ax} r^3 dr}{3V} \quad (5)$$

If c_{ax} were constant throughout the inlet cross section, we would then have $V = c_{ax} 2\pi (r_4^2 - r_3^2)$ and

$$r_{1m}^2 = \frac{1}{2} (r_4^2 + r_3^2) \quad (6)$$

The axial inflow velocity is not constant, however. Since the air flows from the entrance spiral, the velocity at the point of maximum deflection of the streamlines, i.e., at the maximum inlet diameter, is the highest and at the minimum deflection of the streamlines, i.e., at the minimum inlet diameter, it is the lowest. The calculation of the velocity distribution over the inlet cross section might still be very difficult, due to the influence of the inlet guide vanes. Moreover, due to the sharp bend in the vicinity of the maximum inlet diameter, no potential flow can be expected. It is therefore assumed, as an approximation, that the velocity increases in proportion to the inlet radius according to

$$c_{ax} = k_1 r_1 \quad (7)$$

Introduced into equation (5), this yields

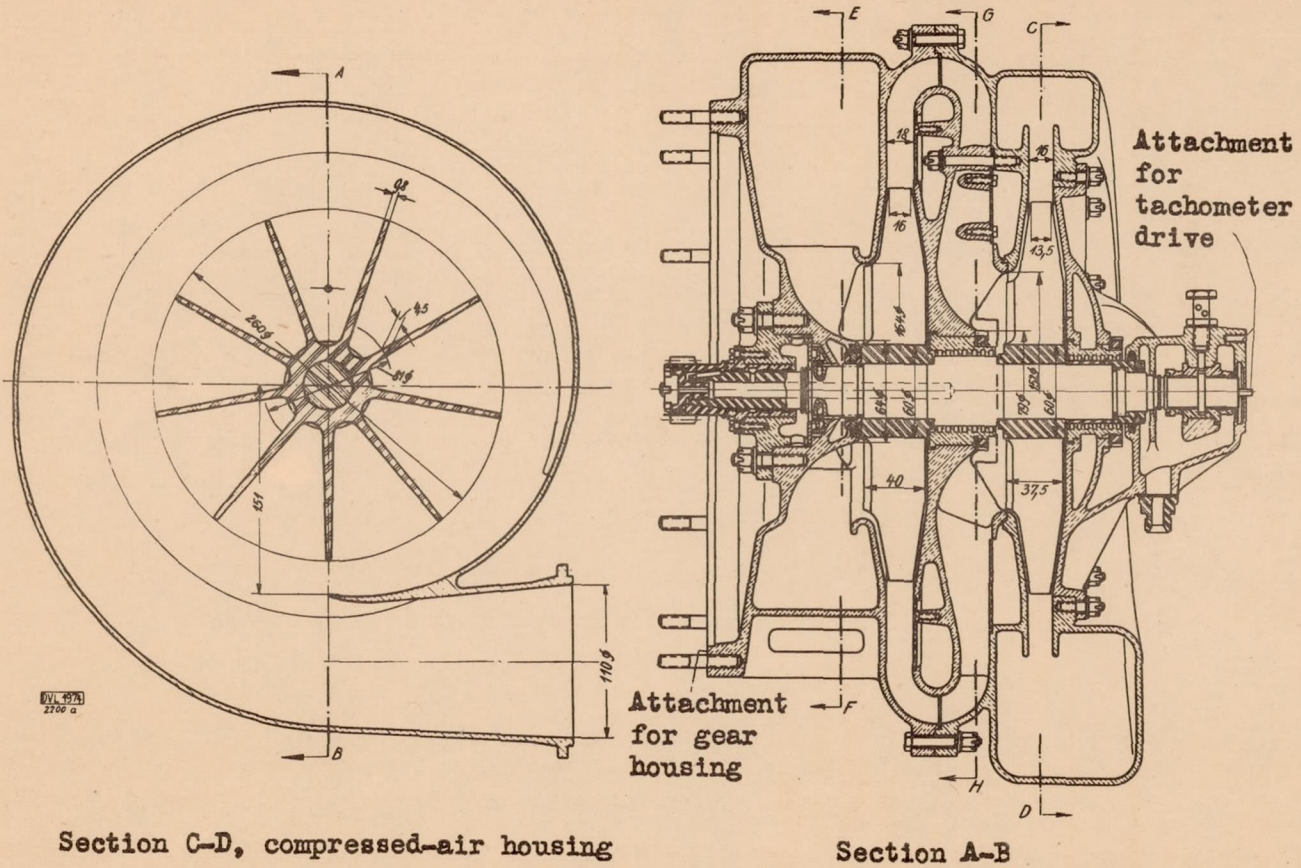
$$r_{1m}^2 = \frac{3}{5} \times \frac{r_4^5 - r_3^5}{r_4^3 - r_3^3} \quad (8)$$

For r_{1m} we obtain:

	Stage 1	Stage 2
According to equation (8)	65.2 mm	61.3 mm
" " " (6)	62.3 "	59.3 "

The difference in the values of r_{1m} , under the given assumptions for the velocity distribution is therefore not very large. It may be assumed that the actual value of r_{1m} differs still less from that calculated according to equation (8).

Translation by Dwight M. Miner,
National Advisory Committee
for Aeronautics.



Section C-D, compressed-air housing

Section A-B

Figure 1.-Longitudinal section and section through compressed-air housing.

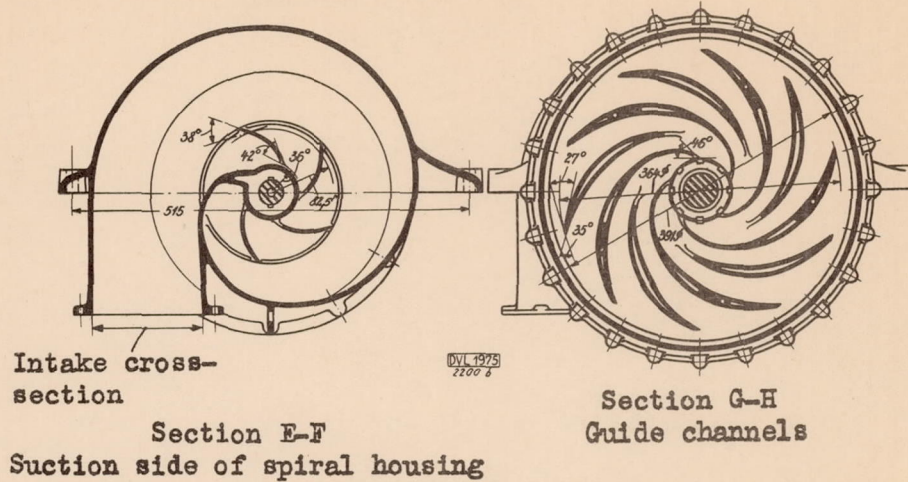


Figure 2.-Inlet spiral and guide channels.

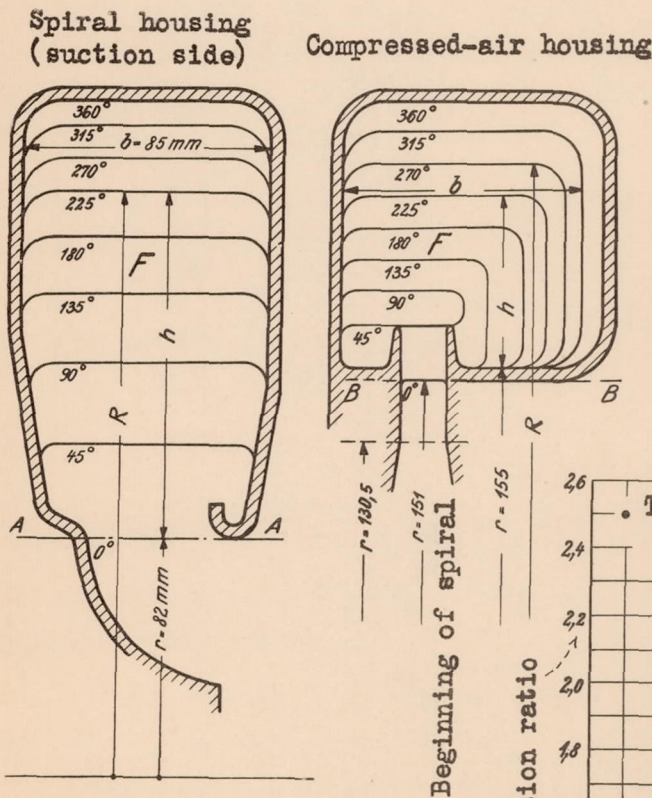


Figure 3.-Cross sections of inlet and outlet spirals.

(For dimensions see table on following page.)

Figure 8.-Work diagram of super-charger for a room temperature of 20°C and a final pressure of 760 mm Hg.

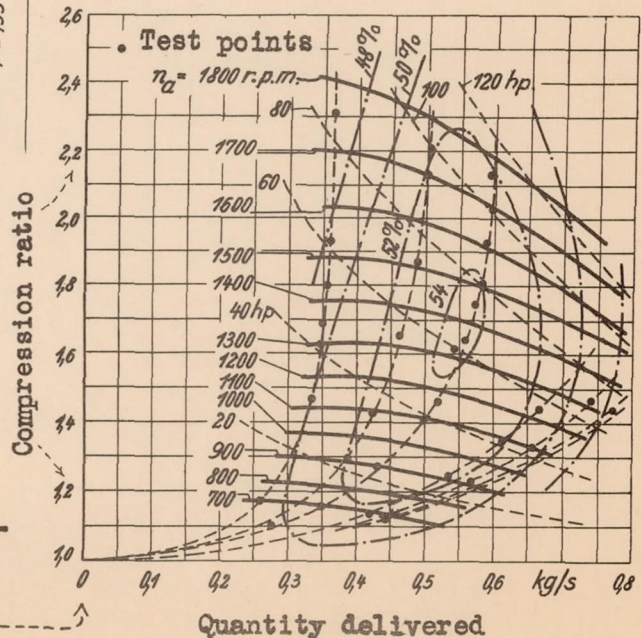


Figure 3 (continued)

Location of section degrees	Housing of spiral			Compressed-air chamber			
	Inside dimensions		Section A-A cm ²	Inside dimensions			Section B-B cm ²
	h mm	R mm		h mm	R mm	b mm	
0	0	82	F = 0	0	155	-	F = 0
45	32	114	21.0	15	170	-	4.6
90	60	142	44.2	26.5	181.5	42	10.1
135	84	166	63.2	37	192	50	18.0
180	103	185	79.8	48	203	62	29.2
225	118	200	93.4	59	214	70	40.5
270	129.5	211.5	102.5	70	225	76	51.8
315	141	223	112.4	81	236	82	65.4
360	150	232	118.5	92	247	90	80.8

Inlet section

$145 \times 85 \text{ mm} = 123 \text{ cm}^2$

Outlet section

$110 \text{ } \phi = 95 \text{ cm}^2$

$\text{mm} \times 0.03937 = \text{in.}$

$\text{cm}^2 \times 0.155 = \text{sq.in.}$

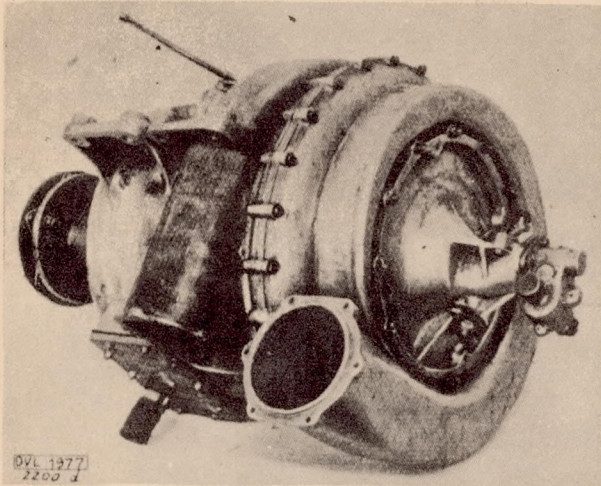


Figure 4.-
Supercharger
with
driving
gear.

Figure 5.-
Supercharger
and gear
separated.

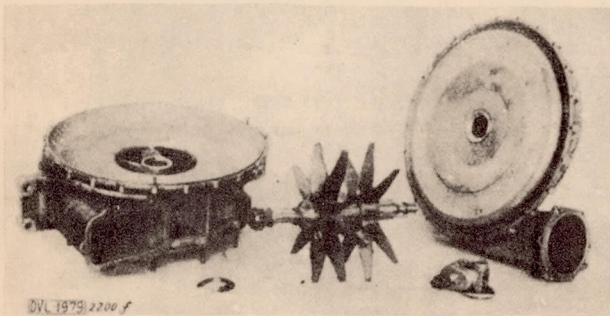
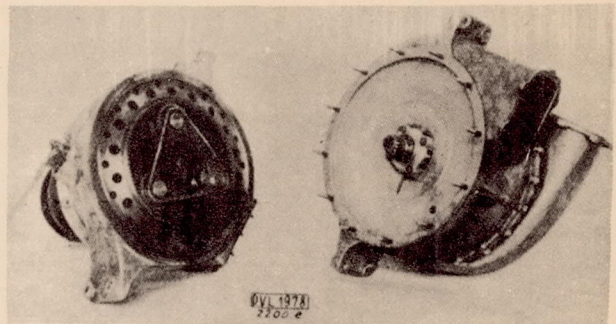
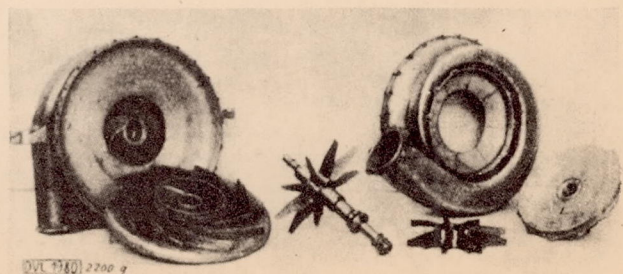


Figure 6.-
Details
of
supercharger.

Figure 7.-
Details of
supercharger
(further
separated).



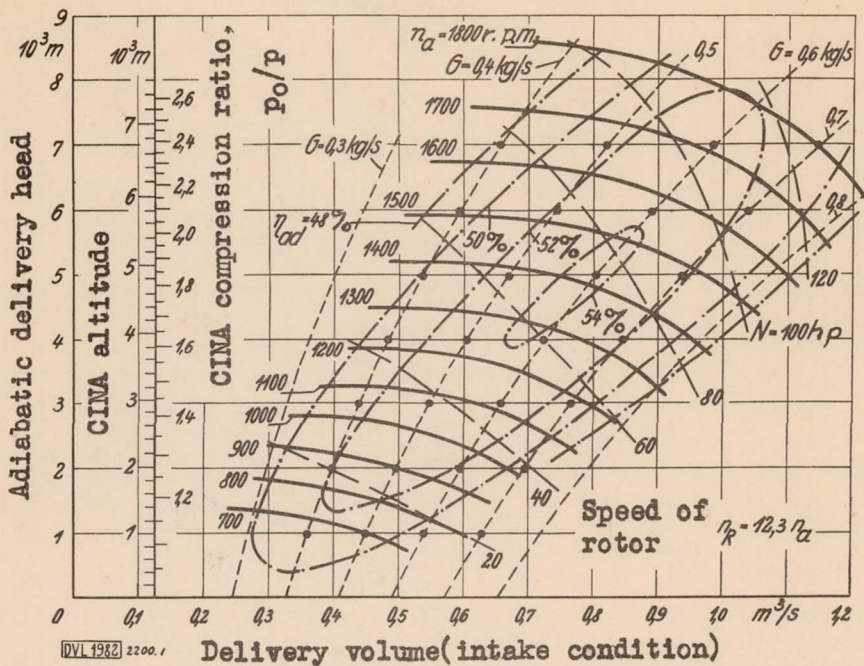


Figure 9.-
Work
diagram
of
supercharger.

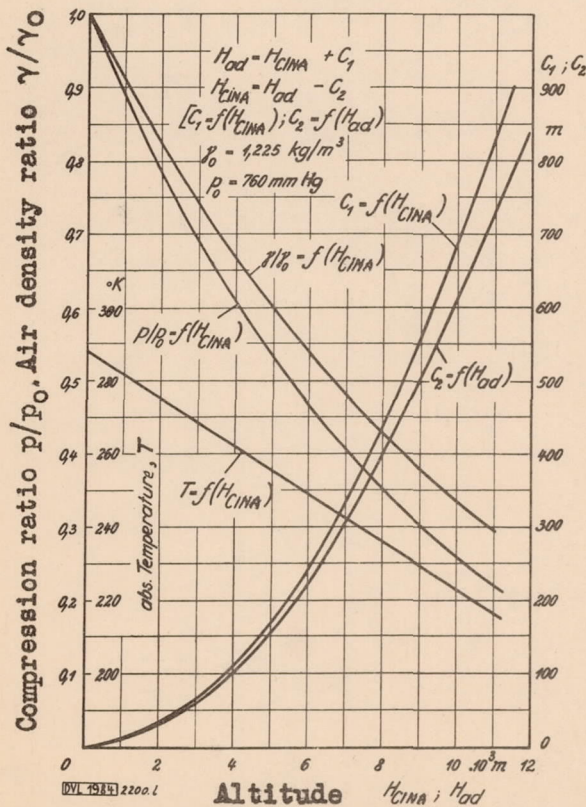


Figure 11.-Relation between CINA constant-pressure altitude and requisite adiabatic delivery head for attaining this altitude. Air temperature, pressure and density plotted against altitude in CINA atmosphere.

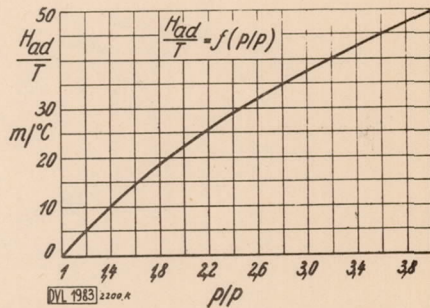


Figure 10.-Diagram for finding compression ratio from adiabatic delivery head and intake temperature. Adiabatic exponent $\kappa=1.405$

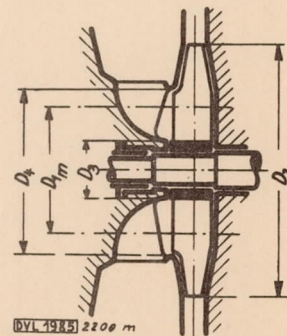


Figure 12.-Determination of mean inlet diameter.